

Role of Iron Vacancies in Pyrrhotite-Catalyzed Liquefaction  
Using  $H_2S$  and CO

J. Nowok and Virgil I. Stenberg

Department of Chemistry, University of North Dakota,  
Grand Forks, North Dakota 58202

INTRODUCTION

As a part of continuing investigations into the chemistry of liquefaction catalyzed by metal sulfides, a study was made of the interaction of  $H_2S$  and CO with the pyrrhotite surface using ESR spectroscopy. Minerals contained in coals are reported to promote hydrogenation and hydrodesulfurization in low-rank coal conversion processes (1,2). More specifically, those containing iron are found to promote both hydrogenation and desulfurization reactions (3). In the pyrite and pyrrhotite forms, iron has hydrogenation activity (4-6). The liquefaction activities of iron sulfides in the absence of added  $H_2S$  are distinguished by sulfur concentration and shown to be  $FeS_2 > Fe_2S_3 > Fe_{1-x}S > FeS$  (7). However, pyrite quickly decomposes to pyrrhotite at liquefaction temperatures (8,9). Consequently, the catalytic activity of iron sulfides is attributed to a combination of pyrrhotite and  $H_2S$  (10,11).

Transition metal-catalyzed hydrodesulfurization has been related to the ability of these to form and regenerate sulfur vacancies (12). The catalyst is also sensitive to the number of metal vacancies (6). The variability of the composition of iron sulfides,  $Fe_{1-x}S$ , found in liquefaction residues is consistent with these conclusions.

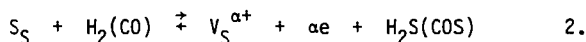
$FeS$  is of the NiAs crystal-type and is a  $d^6$  high-spin quintet state solid with metal properties. In an octahedral field, the d orbitals are split into two energy levels,  $t_{2g}^3$  and  $e_g^3$  (13). The non-stoichiometric crystal-related form of triolite ( $FeS$ ) is pyrrhotite. The latter includes a wide group of iron sulfides,  $Fe_{1-x}S$  with  $0 < x < 0.2$  (14). All form superstructures with ordered iron vacancies and ordered spins (15). The pyrrhotites are formed by either pyrite decomposition with subsequent crystal transformation or sulfur incorporation to  $FeS$  lattice by reaction with sulfur or  $H_2S$ , cf. reaction 1

(16).  $S_S$ ,  $V_{Fe}^{\alpha-}$  and  $h^+$  represent sulfur on its normal lattice position, an  $\alpha$  times ionized iron vacancy, and an electron hole, respectively.



$V_{Fe}$  vacancies create electron acceptor energy levels which, in turn, induce electron transfer from the surrounding lattice sulfur ions. This electron transfer process creates electron deficient orbitals or "holes" (17). For non-stoichiometric sulfides such as,  $Fe_{0.996}S$ , the 3p(S) holes are present in such numbers ( $\sim 10^{20}/cc$ ) that they form an impurity energy level which overlaps in energy with the 3d Fe(II) energy level (21). This gives rise to a large increase in density of states mainly in direction parallel to the C axis (9) and disturbs electrons distribution in  $t_{2g}$  and  $e_g$  levels.

The existence of an active catalytic site is now postulated to be localized on iron ion and its surrounding matrix. The disturbance of the 3d  $Fe^{2+}$  orbital electron distribution brought about by iron vacancies gives rise to the catalytic active centers on the solid surface. Also, there appears to be a secondary catalytic effect connected with formation and regeneration of sulfur vacancies,  $V_S^{\alpha+}$  (12). The latter occur in the sulfur sublattice and are formed according to reaction 2.



## EXPERIMENTAL

### A. Catalyst Preparation

The pyrrhotite received from the coal cleaning operation of the U.S. Steel Robena Mines, Pennsylvania, were ground and sieved through a 200-mesh screen (75  $\mu m$ ). The BET surface area of the catalysts used in experiments ranges between 5 and 8  $m^2/g$  (18).

### B. Liquefaction Procedure

The Big Brown lignite (C, 74.1 wt %; H, 5.4 wt %; N, 1.3 wt %; O, 18.1 wt %; S, 1.1 wt %; Texas) used in the experiments was ground and sieved through a 200-mesh screen. The moisture content was 26.1% as received, and mineral

amount was 9.2%. Approximately 1 g of the coal sample was inserted into the 12-ml tubing reactors constructed of 316-stainless steel. The reactors were additionally charged with catalyst (about 0.15 g), with water (0.8 g) and by gases:  $\text{H}_2\text{S} = 1.75$  MPa,  $\text{H}_2 = 3.5$  MPa and  $\text{CO} = 3.5$  MPa. The liquefaction experiments were carried out at temperatures ranging from 573-773°K for 60 min. Conversion to volatile products was calculated on moisture-ash free (MAF) coal basis after heating samples at 523°K in vacuo ( $\sim 1$  mm Hg) for 5 hrs (19).

### C. ESR Measurements

ESR investigations were performed on powdered pyrrhotite in a vacuum as well as under  $\text{CO}$ ,  $\text{H}_2\text{S}$ , or a  $\text{CO}$  and  $\text{H}_2\text{S}$  mixture over the range of temperature 293-773°K. The pyrrhotite was added into the ESR glass sample tube which was connected with a vacuum line and reactant gas cylinders applied. The vacuum was  $10^{-1}$  torr and that of the gases were 0.05-0.10 MPa each. The samples were outgassing at room temperature for 0.5 hr before introducing the reactant gases. All ESR spectra were recorded using a Bruker ER-420 spectrometer employing 100-kHz modulation with a resonance frequency 9.86 GHz. A polycrystalline sample of DPPH ( $g = 2.0036$ ) was used as a  $g$ -marker when investigations were performed at room temperature.

## RESULTS

### 1. Catalysis of BB1 Lignite Hydroliquefaction by Iron Sulfide Catalysts

In a previous article (19), the conversion of BB1 into volatile products in the  $\text{H}_2\text{S}-\text{H}_2\text{O}-\text{H}_2-\text{CO}$  system with no added catalyst was reported to be temperature dependent. Using the same experimental conditions, pyrrhotite was shown to increase the conversion into distillate of BB1 lignite over the temperature range of 573-773°K with constant 60-minute time (Figure 1) and the time range of 0-60 minutes with constant 420°C reactor temperature (Figure 2). The latter conversion results followed the equation,  $\text{conversion} = k \ln t$  where  $k$  is conversion coefficient and  $t$  is time. Pyrrhotite is more active with  $\text{CO}-\text{H}_2\text{S}-\text{H}_2\text{O}$  than with  $\text{H}_2-\text{H}_2\text{S}-\text{H}_2\text{O}$  (Figure 3). Under the reactor conditions at 693°K for 1 hr but in the absence of coal, the conversion of  $\text{CO}$  into  $\text{CO}_2$  with added  $\text{H}_2\text{S}$  was equal to 5.3%. Using pyrrhotite at the same experimental conditions, it was 6-fold greater (31.7%).

## 2. Electron Spin Resonance Spectra of Non-stoichiometric Iron Sulfides

### A. Pyrrhotite-H<sub>2</sub>S-CO System

The ESR spectrum of Fe<sub>1-x</sub>S contains a broad resonance signal and a narrow resonance signal in the 3.10 g region (Figure 4). The latter is the focus of attention herein and is assigned to high spin iron(II) in its surrounding matrix (20). The spectra are recorded either in vacuum (Figure 4a), H<sub>2</sub>S (Figure 4b), or CO (Figure 4c). The signal is split into two in vacuum at 388°K, with H<sub>2</sub>S at 293°K, and with CO at 408°K. Both the relative intensities of the two signals (A and B) and their g-values are temperature dependent (Figure 5). Above 593-663°K, the CO-pyrrhotite signal becomes reversibly broadened. The CO-pyrrhotite ESR signal change is modified by the presence of H<sub>2</sub>S (Figure 5). The signal changes are reversible.

## DISCUSSION

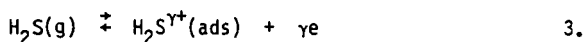
The liquefaction yields of distillate products are markedly improved in the presence of pyrrhotite as opposed to those reactions done in its absence. These data suggest that chemisorption occurs between the reacting gases and the pyrrhotite. The principal purpose of this study is to obtain direct evidence for this interaction. The ESR technique is used as the principal tool.

The sharp ESR signal of pyrrhotite in vacuum demonstrates the paramagnetic behavior of the Fe(II) ion in its solid matrix. This Fe(II) ESR signal splits into two, A and B, above 388°K (Figure 4a). The new ESR signals are now assigned to be a consequence of an electron transfer process in the solid matrix. Specifically, electrons are believed to be transferred from sulfide, S<sup>-2</sup>, into the iron vacancy, V<sub>Fe</sub><sup>α-</sup>. The reduced charged S<sup>2-</sup> which is formed is electronegative, i.e., it has a hole (ah<sup>+</sup>). The crystal field is changed with the consequence of changes in the spin intrinsic magnetic moment of the nearest neighbor cations so the two spin couplings of the shifted orbitals are induced. An interaction between the sulfide hole and paramagnetic iron ion occurs which gives rise to peak A. The weaker interaction between the trapped electron on iron vacancy and paramagnetic iron ion moment gives rise to peak B.

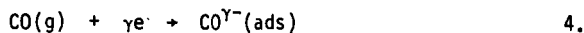
The changing g-values of ESR peaks A and B with four conditions as the temperature is increased are shown in Figure 5. The g-value variation of peaks

A and B with temperature indicate changes in the crystal electric field. These values are dependent upon the electron transfer between the adsorbate and the adsorbent.

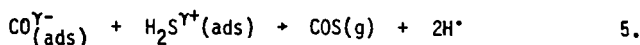
Upon exposure of pyrrhotite to  $H_2S$  at room temperature, the  $Fe^{2+}$  ESR signal is split into two separate ones (Figure 4b). Peak B resides at larger g-values (Figure 4b). This gives direct evidence for chemisorption of the  $H_2S$  onto the surface. Since the dominant chemical feature of  $H_2S$  is the electron rich sulfur and the  $H_2S^+$  molecular cation was recently reported (22), the chemisorption process is interpreted as the occurrence of charge transfer from the electron rich  $H_2S$  onto the pyrrhotite surface (reaction 3). The free electrons formed by this means are delocalized into the iron vacancy band probably throughout 3d  $Fe^{2+}$  band.



CO, in contrast to  $H_2S$ , is ordinarily an electron acceptor in charge transfer processes. At room temperature, its presence does not alter the sharp ESR signal of pyrrhotite. However, the signal is significantly split and altered with increasing the temperature (Figure 5). This g-value variation is assigned to  $CO^-$  species formed after electron transfer from iron vacancy band, reaction 4 (23-25). The intensity of peak A is more altered than peak B by the presence of CO.



The summary significance of the reactions 3 and 4 is that hydrogen sulfide and carbon monoxide are both activated by the pyrrhotite surface to chemically react according to equation 5. When CO and  $H_2S$  are together in the presence of pyrrhotite, peak A is little altered with temperature. This is consistent with reactions 3 and 4 simultaneously occurring on the pyrrhotite surface resulting in the production of COS (reaction 5). The active hydrogen,  $H_1$ , is consumed by the liquefaction media.



Under high  $H_2S$  partial pressures in the reactor, the Mössbauer Spectrum (18) showed the presence of  $FeS_2$ .  $FeS_2$  is much reduced if not absent when the partial pressure of  $H_2S$  is reduced. Therefore, the production of COS by  $CO + H_2S$  occurs together with the transformation of  $Fe_{1-x}S$  into  $FeS_2$ .

#### ACKNOWLEDGEMENT

We are grateful for the financial support of the United State Department of Energy.

#### REFERENCES

1. J.A. Guin, A.R. Tarrer, J.M. Lee, L. Lo and Ch.W. Curtis, *Ind. Eng. Chem. Process Des. Dev.* **18**, 371 (1979).
2. J.A. Guin, A.R. Tarrer, J.W. Prather, D.R. Johnson and J.M. Lee, *Ind. Eng. Chem. Process Des. Dev.* **17**, 118 (1978).
3. A. Attar, *Fuel* **57**, 201 (1978).
4. R.M. Baldwin and S. Vinciguerra, *Fuel* **62**, 498 (1983).
5. D. Garg and E.N. Givens, *Ind. Eng. Chem. Process Des. Dev.* **21**, 113 (1982).
6. P.A. Montano and B. Granoff, *Fuel* **59**, 214 (1980).
7. S. Yokoyama, H. Narita, T. Yoshida, R. Yoshida, Y. Hasegawa and Y. Maekawa, *Symp. on Chem. Coal Liquef. and Catalysis*, Hokkaido Univ., March 17-20, 1985, Sapporo 060, Japan, p. 155.
8. A.S. Bommannavar and P.A. Montano, *Fuel* **61**, 523 (1982).
9. P.J. Cleyle, W.F. Caley, I. Stewart and S.G. Whiteway, *Fuel* **63**, 1579 (1984).
10. P.A. Montano and V.I. Stenberg, *Proceedings, 1985 National International Conference on Coal Science*, Sidney, Australia, 788-791.
11. V.I. Stenberg, T. Ogawa, W.G. Wilson and D. Miller, *Fuel* **62**, 1487 (1983).
12. T.A. Pecorano and R.R. Chianelli, *J. Catal.* **67**, 430 (1981).
13. T.A. Bither, R.J. Bouchard, W.H. Cloud, P.C. Donohue and W.J. Siemons, *Inorg. Chem.* **7**, 2208 (1981).
14. D.J. Vaughan and J.R. Craig, *Mineral Chemistry of Metal Sulfides*, Cambridge Univ. Press, Cambridge, 1978, p. 12.
15. E.F. Bertaut, *Acta Cryst.* **6**, 557 (1953).
16. F.A. Kroger, *The Chemistry of Imperfect Crystals*, North-Holland, Amsterdam, 1964.
17. L.A. Marusak and L.L. Tongson, *J. Appl. Phys.* **50**, 4350 (1979).
18. P.A. Montano, V.I. Stenberg and P. Sweeny, *J. Phys. Chem.* **90**, 156 (1986).
19. V.I. Stenberg and J. Nowok, *Fuel* accepted for publication.
20. W. Low and E.L. Offenbacher, *Solid State Physics* (ed by F. Seitz and D. Turnbull) **17**, 135 (1965).
21. S.L. FinkTea III, Cathey LeConte and E.L. Amma, *Acta Cryst.* **A32**, 529 (1976).
22. Ibuki Toshio, *J. Chem. Phys.* **81**, 2915 (1984).
23. P.C. Stair, *J. Am. Chem. Soc.* **104**, 404 (1982).
24. R.J. Madrix and J. Benziger, *Ann. Rev. Phys. Chem.* **23**, 285 (1978).
25. L.H. Dubois and B.R. Zegarski, *Chem. Phys. Lett.* **120**, 537 (1985).

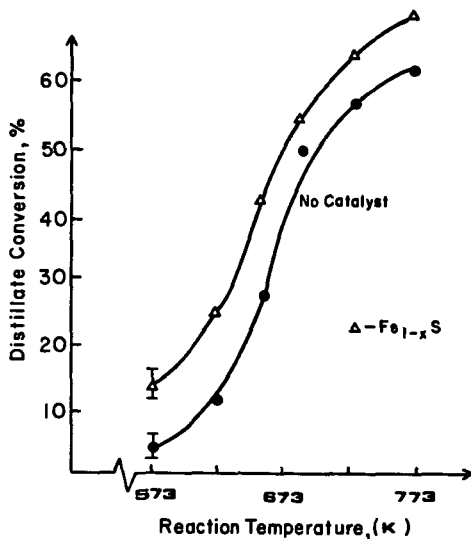


Figure 1. The effect of temperature on catalytic liquefaction of BB1 lignite in  $H_2S-H_2-CO-H_2O$  system. The time of the reaction was 1 hr. The pressures of the gases were:  $H_2S$ , 1.75 MPa;  $H_2$ , 3.5 MPa; and  $CO$ , 3.5 MPa. Water (0.8 g) was added.

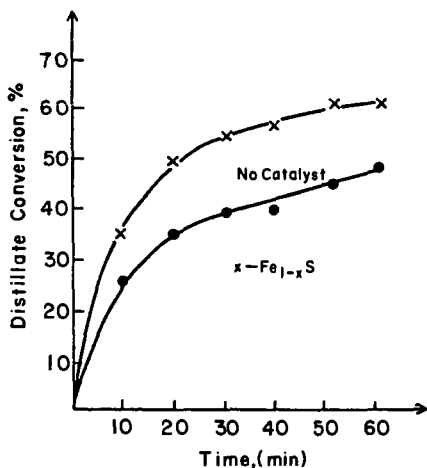


Figure 2. Kinetics of BB1 lignite liquefaction at 693 K with and without catalyst in  $H_2S-H_2-CO-H_2O$  system. The temperature of the reaction was 420°C, and the rest of the contents were those given for Figure 1.

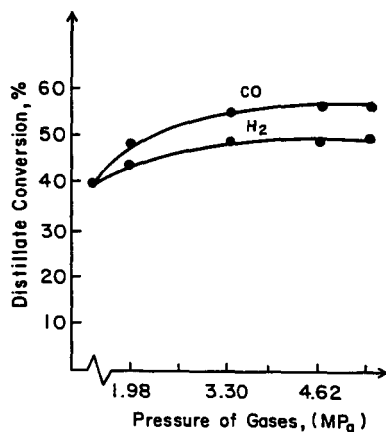


Figure 3. The effect of  $H_2$ - $H_2S$ - $H_2O$  and  $CO$ - $H_2S$ - $H_2O$  on conversion yields. The liquefaction reactions were performed at 693 K for 1 hr with water = 0.8 g and  $H_2S = 1.75$  MPa.

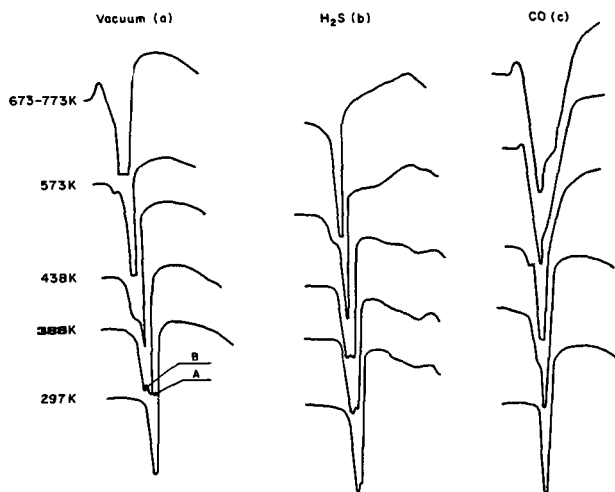


Figure 4. ESR signal of high spin iron (II) with  $g = 3.10$  detected in vacuum (a),  $H_2S$  (b) and  $CO$  (c) at the range of temperatures 293-773 K.

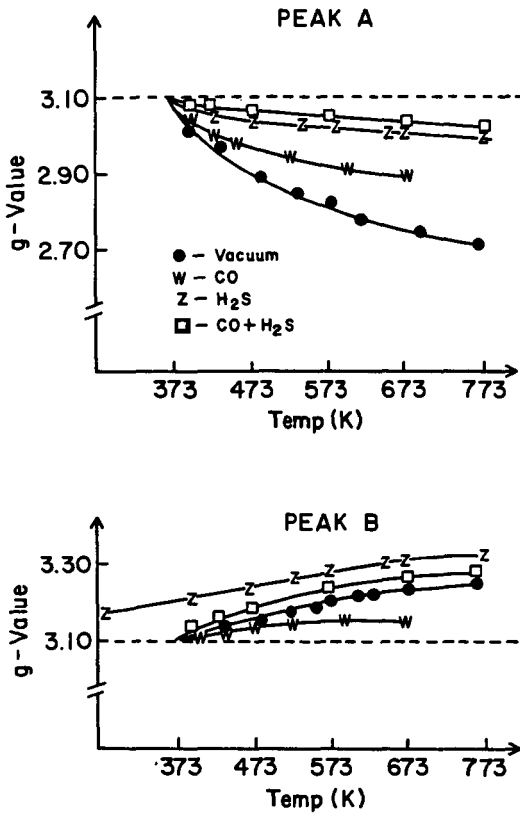


Figure 5. The variation of g-values of splitting  $Fe^{2+}$  signal detected in vacuum,  $H_2S$ , CO and  $H_2S + CO$  gases.